Purdue University
Purdue e-Pubs

International Refrigeration and Air Conditioning Conference

School of Mechanical Engineering

2018

Impact of Liquid/Vapor Maldistribution on the Performance of a Plate Heat Exchanger Evaporator for Pure and Mixed Refrigerants

Roberta Mancini
Section of Thermal Energy, Departement of Mechanical engineering, Technical University of Denmark, Nils Koppels Allé 403, Kgs. Lyngby, 2800, Denmark, robman@mek.dtu.dk

Vikrant Chandramohan Aute
University of Maryland College Park, vikrant@umd.edu

Wiebke Brix Markussen
Section of Thermal Energy, Departement of Mechanical engineering, Technical University of Denmark, Nils Koppels Allé 403, Kgs. Lyngby, 2800, Denmark, wibr@mek.dtu.dk

Brian Elmegaard
Section of Thermal Energy, Departement of Mechanical engineering, Technical University of Denmark, Nils Koppels Allé 403, Kgs. Lyngby, 2800, Denmark, be@mek.dtu.dk

Follow this and additional works at: https://docs.lib.purdue.edu/iracc

Mancini, Roberta; Aute, Vikrant Chandramohan; Brix Markussen, Wiebke; and Elmegaard, Brian, "Impact of Liquid/Vapor Maldistribution on the Performance of a Plate Heat Exchanger Evaporator for Pure and Mixed Refrigerants" (2018). *International Refrigeration and Air Conditioning Conference.* Paper 1891.
https://docs.lib.purdue.edu/iracc/1891

Impact of Liquid/Vapor Maldistribution on the Performance of a Plate Heat Exchanger Evaporator for Pure and Mixed Refrigerants

Roberta MANCINI[1]*, Vikrant AUTE[2], Wiebke BRIX MARKUSSEN[1], Brian ELMEGAARD[1]

[1]Section of Thermal Energy, Department of Mechanical Engineering,
Technical University of Denmark, 2800 Kongens Lyngby, Denmark
Tel: +45 4525 4161, Fax: +45 4525 1961,
Emails: robman@mek.dtu.dk*, wb@mek.dtu.dk, be@mek.dtu.dk

[2]Center for Environmental Energy Engineering,
Department of Mechanical Engineering, University of Maryland,
College Park, MD 20742, USA
Email: vikrant@umd.edu

* Corresponding Author

ABSTRACT

This paper presents an estimation of the degradation in heat transfer performance in plate heat exchanger (PHE) evaporators due to flow maldistribution. A booster heat pump system integrated in a district heating network is used as a case study. Butane and two zeotropic mixtures, namely Propylene/Butane (0.5/0.5) and R1234yf/R1233zdE (0.5/0.5) were evaluated as working fluids. A two-dimensional (2D) numerical model was developed for the evaluation of the total heat flow rate degradation due to the imposed uneven liquid/vapor distribution at the inlet of the PHE channels. Butane showed the largest sensitivity to both the effect of end plates and maldistribution, with an overall reduction of the heat flow rate equal to - 11.2 %. Both the zeotropic mixtures were only insignificantly affected by the uneven quality distribution at the inlet, and suffered a slight reduction of the overall heat flow rate of - 0.9 % and - 0.8 % respectively, due to effect of end plates. Last, the sensitivity to the boundary conditions of the case study was assessed for the mixture Propylene/Butane (0.5/0.5), evaluating the dependence of the obtained results from superheat and number of channels, since both parameters impact the degradation of heat transfer performance.

1. INTRODUCTION

Plate heat exchangers (PHEs) have been increasingly employed in a range of different applications, such as food, chemical and process industries, as well as in the energy sector. They are widely used as evaporators and/or condensers for refrigerating cycles and heat pumps, thus constituting a key component for cycle design and optimization. PHEs are comprised of thin parallel plates stacked together to form parallel channels for fluid flow, which can be arranged in co- or counter-current configurations. The typical chevron corrugation of the plates allows achieving high heat transfer coefficients within a compact design, constituting the key-advantage compared to other heat exchanger (HEX) configurations (Shah and Sekulic, 2002). The occurrence of flow maldistribution can however degrade the performance of multiple channels HEXs. Mueller and Chiou (1988) conducted an extensive review on the main causes of maldistribution, which can be induced by fluid flow characteristics (two-phase flow), fouling, corrosion and nozzle design. It is therefore of paramount importance to estimate the impact of maldistribution on the performance of PHEs.

Bassiouny and Martin (1984a, 1984b) studied the uneven distribution of liquid-to-liquid PHEs for both U-type and Z-type flow arrangements by an analytical model, proposing to compensate the effect by tuning the area ratio between inlet and outlet fluid ports. Rao and Das (2004) studied the maldistribution effect on fluid pressure drop for a PHE for single-phase applications experimentally. Rao et al. (2005) further studied the effect on PHE thermal performances and they found that the deterioration of heat transfer and increase of pressure losses were affected by port size, number of channels, and mass flow rate. Srihari et al. (2005) and Srihari & Das (2006) developed analytical models based on the work of Bassiouny and Martin (1984a, 1984b), in order to study the transient response of PHEs in single pass and multi-pass configurations, showing how flow maldistribution affected the performance of the component in both

steady state and transient operations. Further works by Bobbili et al. (2006) and Tereda et al.(2007) demonstrated the occurrence of flow maldistribution in U-type configuration PHEs experimentally, with more severe maldistribution occurring for higher mass flow rates, smaller port diameters and higher number of channels. Their experimental results showed a good agreement with the analytical treatment first developed by Bassiouny and Martin (1984a, 1984b). Li and Hrnjak (2016) assessed the impact of flow maldistribution of upward nitrogen flow experimentally, using the results to validate a Computational Fluid Dynamics (CFD) model of the PHE header, while Jin and Hrnjak (2017a) evaluated the overestimation of the PHE heat transfer coefficient when the end plate effect is not considered.

Literature reports a limited number of studies focusing on two-phase flow maldistribution in PHEs. Vist and Pettersen (2004) investigated two-phase flow distribution in HEX manifold experimentally, dividing the mass flow into ten channels, in both upward and downward flow configurations. The occurrence of uneven quality distribution was detected for different mass flow rates, resulting in large differences between the thermal load of the various channels. They observed that the vapor phase distributed more easily in the first channels for upward flow, while higher quality was detected in the last channels for downward flow arrangement. Jensen et al. (2015) assessed the impact of such maldistribution by a numerical model, imposing different rates of linear quality variation at the PHE channels inlet. The study was conducted for an evaporator using R134a as working fluid, resulting in a 25 % reduction of the overall heat transfer coefficient when a severe rate of maldistribution was imposed. Jin and Hrnjak (2017b) investigated the distribution of R245fa in a plate channel experimentally, showing large non-uniformities of the flow, heat transfer affected by local heat flux, and occurrence of dry-out zones.

The present work aims at investigating the impact of uneven quality distribution at the inlet channels of PHEs using further numerical modeling. An evaporator of a booster heat pump system for ultra-low temperature district heating (DH) systems is used in the analysis. Zühlsdorf et al. (2018) optimized the coefficient of performance (COP) of the heat pump for different pure fluids and zeotropic mixtures. Due to the non-isothermal nature of mixture phase-change, it is possible to reduce the heat transfer irreversibility in the heat exchangers, by matching the refrigerant temperature profile with the heat source and sink temperature glides. The use of zeotropic mixtures entails however a degradation of the heat transfer coefficient compared to pure fluids (Radermacher and Hwang, 2005), as well as requiring larger heat transfer area for the HEX. The objective of this work is to assess the impact of uneven liquid/vapor distribution imposed at the PHE inlet during evaporation for both pure fluids and zeotropic mixtures.

2. METHODS: CASE STUDY AND MODELLING

2.1 Case study
The assessment of flow maldistribution was carried out for a PHE evaporator for a booster heat pump, for preparation of domestic hot water in ultra-low temperature district heating systems, presented in (Zühlsdorf et al., 2018). A single-stage vapor compression heat pump was suggested for increasing the temperature of one part of the DH forward water stream from 40 °C up to 60 °C, with a total thermal load of 13.9 kW at the condenser. The evaporator heat source (secondary fluid), was taken from the forward DH stream, entering the HEX at 40 °C and then discharged to the return DH line at 25 °C. Different pure and mixed refrigerants were analyzed and ranked with respect to the system COP. The screening was based on a number of natural refrigerants and hydrofluoroolefins (HFOs). Butane, a mixture of Propylene/Butane at 0.5/0.5 mass composition and a mixture of R1234yf/R1233zdE at 0.5/0.5 mass composition were found to be among the best performing fluids, and hence were chosen for the present study. The boundary conditions of the PHE evaporator are reported in Table 1.

Table 1: Evaporator design conditions and COP for the considered working fluids (Zühlsdorf et al., 2018)

Working fluid	$\dot{Q}_{eva}$, kW	p_{eva}, bar	T_{bubble}, °C	T_{dew}, °C	$\dot{m}_{ref}$, kg/s	$\dot{m}_w$, kg/s	ΔT_{sh}, K	$\dot{V}_{out}$, m³/h	COP, -
Butane	11.6	2.25	22.5	22.5	0.0360	0.1857	5	23.1	6.15
Propylene/Butane (0.5/0.5)	12.3	6.29	19.8	37.0	0.0373	0.1967	0	9.9	8.85
R1234yf/R1233zdE (0.5/0.5)	12.3	3.67	18.9	37.3	0.0796	0.1967	0	15.0	8.87

2.2 Plate heat exchanger geometry
The thermodynamic variables at the design point shown in Table 1 were used in order to conduct preliminary sizing of the PHEs for the different working fluids. Each fluid requires a different heat transfer area and thus leads to a

different design. The plate geometry was obtained from a commercial manufacturer and was fixed for all heat exchangers. The total number of channels was determined to meet the design thermal load for all the fluids. The design specifications are reported in Table 2 with the chosen PHE plate size, defined by plate width W and length L. The PHE was assumed to be constructed in stainless steel, with a thermal conductivity equal to 16.2 W(mK)^{-1}. Moreover, the PHEs were designed to operate with counter-current flow arrangement, which is essential to achieve the temperature glide match between the mixtures and the secondary fluid.

Table 2: Evaporator SWEP V80 (SWEP International AB, 2015) plate dimensions and count

W, m	L, m	$N_{ch_{tot}}$,-		
		Butane	Propylene/Butane (0.5/0.5)	R1234yf/R1233zdE (0.5/0.5)
0.117	0.524	23	49	57

As shown in Table 2, the sizing led to a very different number of required channels for the pure fluid case compared to the two zeotropic mixtures. A higher heat transfer area is required for the lower mean temperature difference during evaporation due to mixture glide and to account for the heat transfer degradation compared to pure fluids.

2.3 Imposed vapor quality maldistribution

The uneven vapor quality maldistribution was imposed and used as input to the PHE numerical model. Vist and Pettersen (2004) showed that the vapor phase distribution changed monotonically with increasing distance from the inlet manifold, depending on the flow direction (upward or downward). A linear variation of the vapor quality at the inlet of the channels was therefore assumed, similar to (Jensen et al., 2015). The variation was imposed by a vapor quality difference parameter Δx, indicating the absolute difference between the vapor quality in the first and last refrigerant channel. The vapor quality at the inlet of the jth channel is hence estimated by Eq. (1):

$$x_{IN_j} = x_{IN_1} + \frac{j-1}{N_{ch_{ref}}-1} \Delta x \tag{1}$$

x_{IN_j} was expressed as function of the total number of refrigerant channels $N_{ch_{ref}}$ and of the inlet vapor quality at the first channel x_{IN_1}. The study was carried out for different quality difference values ranging from 0.00 up to 0.25 with steps of 0.05. When Δx is equal to zero, a uniform quality distribution is assumed and the mass flow of both refrigerant and secondary fluid is solely affected by the end plates.

2.4 Heat pump boundary conditions

With the occurrence of flow maldistribution, the PHE operation shifts from design conditions. In practical applications, the operating conditions of the refrigerant are adjusted in order to respect the control values. According to the case study boundary conditions (Zühlsdorf et al., 2018), the suction volume flow rate at the evaporator outlet and the refrigerant superheat were fixed to the design values, reported in Table 1. The refrigerant saturation pressure and mass flow rate were estimated accordingly for each case. Note that a different superheat was imposed for Butane and Propylene/Butane (0.5/0.5). Due to the temperature glide during evaporation, zeotropic mixtures offer the possibility of determining the outlet quality by measuring pressure and temperature as independent variables also in the two-phase region. This implies that superheat may not be necessary for control.

2.5 PHE modeling

The heat transfer and fluid flow were solved by an internal solution procedure based on a two-dimensional (2D) discretization of the PHE. An external solver called the internal 2D PHE model for the solution of the mass flow distribution and operating conditions. They are presented in subsections 2.5.1 and 2.5.2, respectively.

2.5.1 Heat transfer and fluid flow

The internal solver iterated on wall temperatures and refrigerant and secondary fluid pressure drops based on a successive substitution approach. The discretization was applied in 2D: lengthwise along the flow direction and with respect to the different PHE channels. The lengthwise discretization divided the PHE in 50 elements of equal heat transfer area. Each element was further divided into a number of control volumes (CVs) equal to the total number of

channels for the refrigerant and secondary fluid, i.e. $N_{ch_{tot}} = N_{ch_{ref}} + N_{ch_{hs}}$. Each CV was therefore representing either the refrigerant or the heat source flow. The PHE was solved with the following assumptions:

1. steady state;
2. adiabatic end plates
3. no longitudinal conduction through the walls;
4. homogeneous two-phase flow.

Based on a linear distribution of wall temperature guess and uniform pressure drops for both fluids, the momentum and energy balance equations were solved iteratively for each CV. Figure 1 shows the structure of the 2D discretization, together with wall temperature and pressure drops used as iteration variables. The tolerance of the solver was given by a 2-norm of the relative residuals of wall temperature and refrigerant and secondary side pressure drops of 10^{-5}. Fluid thermo-physical properties were evaluated using Coolprop (Bell et al., 2014) for pure fluids and water, and REFPROP (Lemmon et al., 2013) for mixtures.

Empirical correlations were used for the evaluation of local heat transfer coefficients and pressure drops. The two-phase refrigerant heat transfer coefficient was estimated by Amalfi et al. (2016) in case of pure fluids. Collier and Thome (1994) recommended the use of the Silver (1947) and Bell and Ghaly (1973) method for the estimation of the two-phase mixture heat transfer coefficient, in order to take the degradation of heat transfer into account. The method estimates the mixture flow boiling heat transfer coefficient as function of the nucleate boiling, convective boiling and vapor only heat transfer coefficients, evaluated by Cooper (1984), Amalfi et al. (2016) and Martin (1996) correlations, respectively. The Thome and Shakir (1987) correction factor was applied to account for the mixture degradation to the nucleate boiling contribution. The single-phase heat transfer coefficient in the superheated region was estimated by using Martin (1996) correlation for both pure and mixed refrigerants, and it was also applied to estimate the heat source heat transfer coefficient. A smooth transition was ensured at the transition between two-phase and superheated region, by calculating the refrigerant heat transfer coefficient as a weighted interpolation of the two-phase and single-phase contributions. The smoothing was applied to the CVs with local vapor quality included in the interval [0.9, 1]. Pressure drops were computed for both fluids by applying the steady-state momentum equation, considering the contributions of friction, acceleration and gravity. The two-phase frictional pressure drops were assessed by applying the Lockhart and Martinelli (1949) method, with coefficients proposed by Palm and Claesson (2006). The single-phase pressure drop of the superheated refrigerant and of the heat source were estimated by Martin (1996). The acceleration and gravity pressure drops in the two-phase region were calculated by using the void fraction model by Smith (1969) for the estimation of the momentum density and cross section average density.
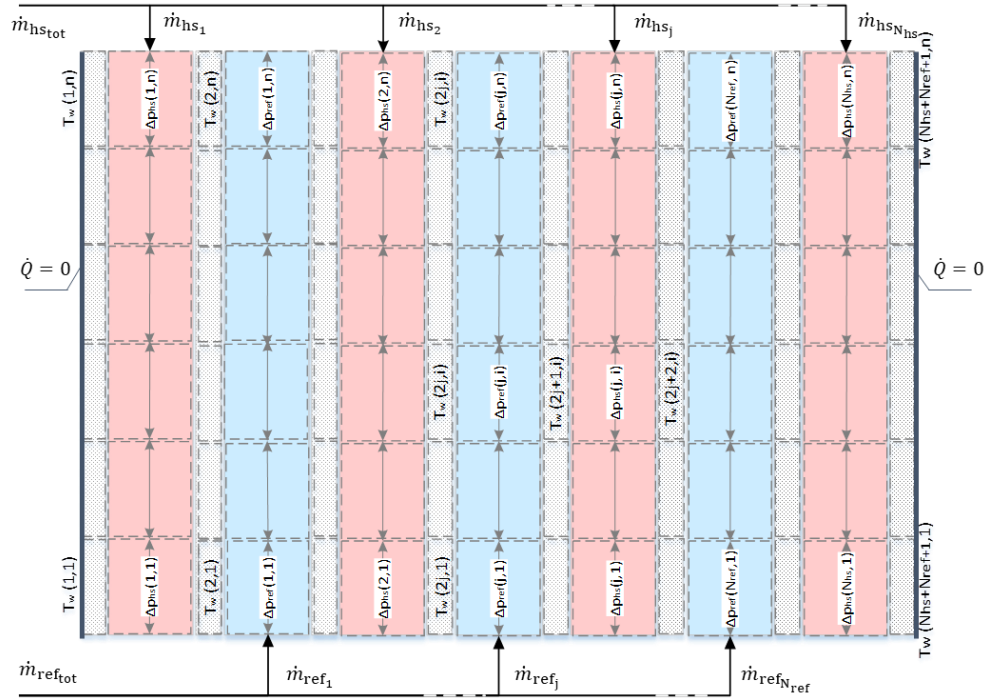

Figure 1: Structure of the discretized 2D PHE model with iteration variables

2.5.2 Solution procedure for flow distribution and operating conditions

The internal solver for heat transfer and fluid flow was coupled with a solver to determine the mass flow distribution of both refrigerant and heat source at the inlet of each channel. The solver determined the refrigerant operating conditions according to the boundary conditions imposed by the cycle, as explained in subsection 2.4. The external solver was based on *fsolve* (Mathworks, 2017), coupled with the user-supplied internal solver for heat transfer and fluid flow. A system of $N_{ch_{ref}} + N_{ch_{hs}} + 3$ equations was therefore solved for the same number of unknowns. The unknowns were the total mass flow rate of the refrigerant, the mass flow rate distribution of both heat source and refrigerant, the refrigerant inlet saturation pressure and the inlet vapor quality of the first channel. The equations are reported in Table 3. The average values of refrigerant temperature and density at outlet conditions were estimated by considering the mixing enthalpy of the refrigerant mass flow from all the channels at the refrigerant outlet pressure.

Table 3: Governing equations of the flow distribution solver

Flow distribution solver governing equations

Mass conservation of manifold

$$\sum_{j=1}^{N_{ch_{ref}}} \dot{m}_{ref_j} = \dot{m}_{ref_{tot}} \qquad \sum_{j=1}^{N_{ch_{hs}}} \dot{m}_{hs_j} = \dot{m}_{hs_{tot}} \qquad \sum_{j=1}^{N_{ch_{ref}}} \dot{m}_{ref_j} x_{ref_{in_j}} = \dot{m}_{ref_{tot}} x_{ref_{in}}$$

Pressure drop equalization

$$\sum_{i=1}^{n} \Delta p_{ref_{i,j}} = \sum_{i=1}^{n} \Delta p_{ref_{i,j+1}} \qquad \sum_{i=1}^{n} \Delta p_{hs_{i,j}} = \sum_{i=1}^{n} \Delta p_{hs_{i,j+1}}$$

$$j = 1, \dots, N_{ch_{ref}} - 1 \qquad\qquad j = 1, \dots, N_{ch_{hs}} - 1$$

Superheat   **Compressor suction volume flow**

$$\bar{T}_{ref_{out}} - T_{dew} = \Delta T_{SH} \qquad\qquad \dot{m}_{ref_{tot}} \cdot \bar{\rho}_{ref_{out}} = \dot{V}_{out}$$

2.5.3 Comparison with one-dimensional (1D) model

In order to separate the effect of uneven vapor quality distribution at the PHE inlet channels from the effect of end plates, the results of the flow distribution solver were compared with a 1D model of the component, discretized along the flow direction. The heat transfer and fluid flow equations were solved iteratively by considering 50 PHE elements, without further discretizing across the PHE channels. The solution procedure was implemented analogously to the 2D model, and the same boundary conditions for superheat and suction volume flow rate were imposed.

2.5.4 Model validation

The 2D heat transfer and fluid flow numerical model coupled with the flow distribution and operating conditions solver was validated against 316 experimental data points for evaporation of R134a, R1234yf and R1234ze (Zhang et al., 2017). The model reported a normalized root mean square error on the total heat flow rate equal to 2.9 % and on the refrigerant pressure drop equal to 23.8 %.

3. RESULTS

3.1 Mass flow distribution and temperature profiles

Figure 2 shows the refrigerant mass flow distribution for the three working fluids at different maldistribution rates, under the design considered in Table 2. The case $\Delta x = 0$ corresponds to the uniform distribution of vapor quality at the inlet channels, wherein the non-uniform mass flow distribution is solely due to the effect of the end plates. The ordinate reports the percentage deviation of the mass flow rate in each channel with respect to the average mass flow rate per channel. The average value is estimated by dividing the total mass flow rate, reported in Table 4 for the different maldistribution cases, by the total number of refrigerant channels. Figure 2 (a) shows that the pure fluid Butane was the most affected by maldistribution, compared to both Propylene/Butane (0.5/0.5) (b) and

R1234yf/R1233zdE (0.5/0.5) (c). The latter was the working fluid being least affected by uneven quality distribution, with maximum differences equal to - 3.3 % for the case of $\Delta x = 0.25$, followed by Propylene/Butane (0.5/0.5) with a maximum deviation of - 6.1 %. Butane showed consistently higher deviations, reaching up to + 46.7 %. Furthermore, Figure 2 reports opposite mass flow trends for the pure fluid compared to the two zeotropic mixtures. In the case of Butane, a higher mass flow rate was obtained in the channels where the inlet vapor quality was lower. This is due to the higher pressure drop entailed by the vapor phase, thereby causing a mass flow reduction in those channels where the complete evaporation and superheat were reached earlier. On the other hand, both Figure (b) and (c) show that the mass flow of the two zeotropic mixtures is only slightly affected by maldistribution. Moreover, Table 4 shows that the total refrigerant mass flow rate of the two mixed refrigerants is only slightly affected by the maldistribution parameter Δx, while the total mass flow of Butane decreases with increasing Δx, thereby implying an expected reduction of the total evaporator heat flow rate.
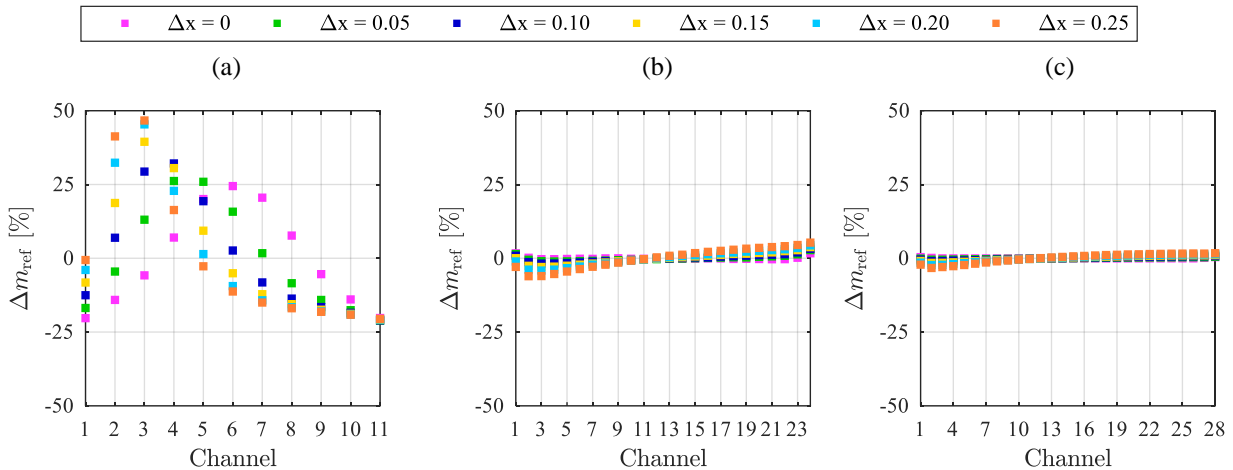

Figure 2: Deviation from average value of refrigerant mass flow rate in each channel at different rates of maldistribution, for (a) Butane, (b) Propylene/Butane (0.5/0.5) and (c) R1234yf/R1233zdE (0.5/0.5)

Table 4: Total refrigerant mass flow rate at different maldistribution rates for the three considered working fluids

Working fluid	$\dot{m}_{\mathrm{ref_{tot}}}$, kg/s					
	$\Delta x = 0$	$\Delta x = 0.05$	$\Delta x = 0.10$	$\Delta x = 0.15$	$\Delta x = 0.20$	$\Delta x = 0.25$
Butane	0.0347	0.0346	0.0344	0.0340	0.0337	0.0334
Propylene/Butane (0.5/0.5)	0.0355	0.0354	0.0354	0.0355	0.0354	0.0354
R1234yf/R1233zdE (0.5/0.5)	0.0745	0.0750	0.0751	0.0750	0.0751	0.0750

The higher sensitivity to maldistribution of the pure fluid can also be observed in the temperature distribution of the refrigerant, heat source and wall temperature in the different channels, which is shown in Figure 3 for the case of severe maldistribution ($\Delta x = 0.25$). The refrigerant flows upward in the even channels, while the water flows downward in the odd ones. Figure 3 (a) shows the results for Butane. The channels with a low refrigerant mass flow rate experienced a large region of superheat, where the temperature level of the refrigerant outlet reached the inlet heat source temperature. The effect on the overall outlet superheat was however compensated by the channels with lower outlet temperature. For instance, incomplete evaporation occurs in channels 4 and 6 of Figure 3 (a), presenting outlet refrigerant temperature equal to the saturation level.

Figure 3 (b) shows the same temperature distribution for the case of Propylene/Butane (0.5/0.5) at $\Delta x = 0.25$. The temperature profiles for R1234yf/R1233zdE (0.5/0.5) were similar to those of Propylene/Butane (0.5/0.5), and hence are not reported here. Compared to the pure fluid, a refrigerant temperature rise can be observed during the evaporation process, due to the characteristic temperature glide of zeotropic mixtures. The effect of end plates can be noticed in the outmost refrigerant channels (channels 2 and 48 of Figure 3 (b)) presenting a slightly higher outlet temperature compared to the inner ones. The effect of maldistribution, namely the slightly uneven mass flow distribution presented in Figure 2 (b), can however not be detected.

(a)   (b)
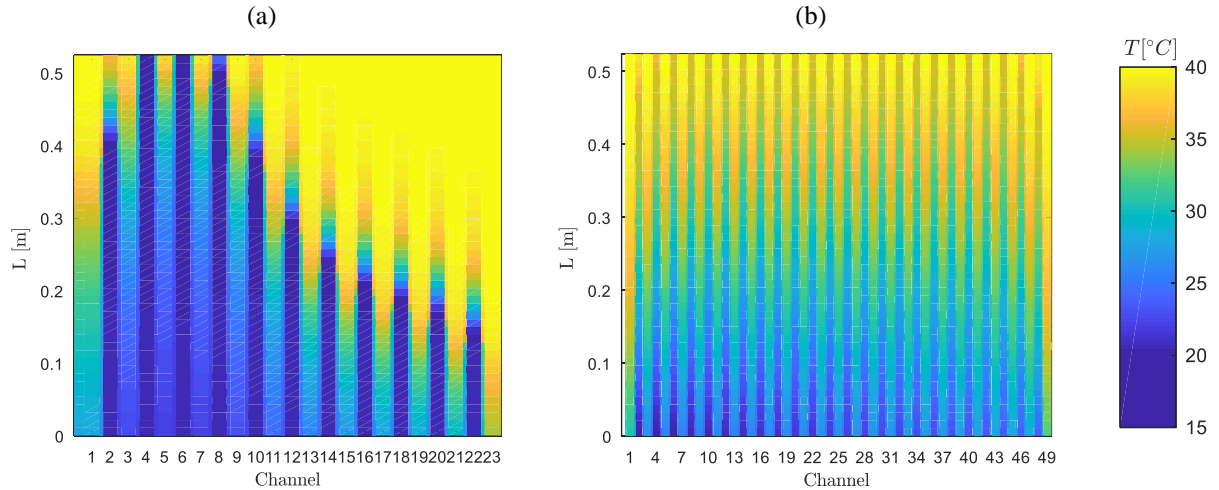
Figure 3: Temperature distribution in the different channel and across the plate length, for (a) Butane and (b) Propylene/Butane (0.5/0.5), for the case of severe maldistribution rate $\Delta x = 0.25$

3.2 Degradation of heat transfer performance

Figure 4 reports the total heat flow rate for the three working fluids as function of the maldistribution parameter Δx. The results are compared with the value obtained by considering a 1D discretization of the PHE along the flow direction, thereby neglecting the effect of end plates. Note that the same boundary conditions on superheat and suction volume were applied to the 1D case. The heat transfer performance for Butane (shown in Figure 4 (a)) was considerably affected by both the effect of end plates and liquid/vapor maldistribution. A reduction of -5.2 % on the total heat flow rate was obtained between the 1D model and the 2D model with $\Delta x = 0$, accounting for the effect of end plates. A further reduction of -6.3 % was obtained between the uniform distribution case and the severe maldistribution imposed by setting $\Delta x = 0.25$.

On the other hand, both zeotropic mixtures Propylene/Butane (0.5/0.5) and R1234yf/R1233zdE (0.5/0.5) (shown in Figure 4 (b) and (c)) report a negligible effect of the liquid/vapor maldistribution on the total heat flow rate, performing with a constant heat flow rate as function of the maldistribution rate Δx. The trend is consistent with the slight impact on the total refrigerant mass flow presented in Table 4. A small effect of the end plates was estimated, equal to a reduction of the heat flow rate of -0.9 % and -0.8 %, for Propylene/Butane (0.5/0.5) and R1234yf/R1233zdE (0.5/0.5), respectively. It must be noted that the lower impact of end plates in the case of the zeotropic mixtures was also affected by a larger number of plates employed by both the designs, namely 49 and 57 against the 23 channels used for Butane.
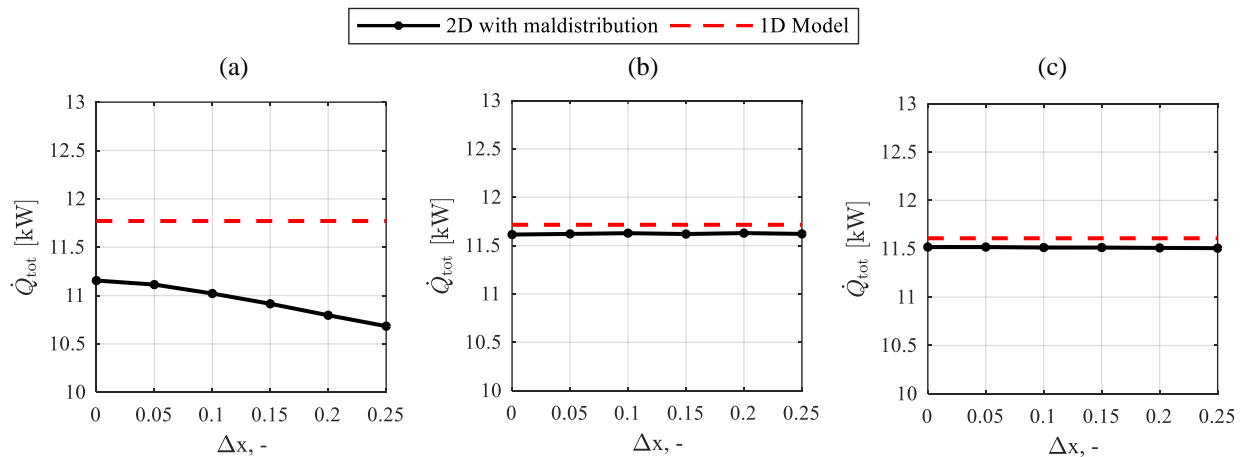
Figure 4: Total heat flow rate as function of the maldistribution rate for (a) Butane, (b) Propylene/Butane (0.5/0.5) and (c) R1234yf/R1233zdE (0.5/0.5)

4. DISCUSSION

5.1 Impact of number of channels and superheat

The results suggest that the zeotropic mixtures may show operating advantages compared to Butane for the heat pump system, due a considerably reduced impact of flow maldistribution on the PHE performance. Despite the higher initial investment for the larger heat transfer area required by the use of mixtures, both Propylene/Butane (0.5/0.5) and R1234yf/R1233zdE (0.5/0.5) were only slightly affected by the occurrence of maldistribution, while Butane suffered from a performance reduction equal to -11.2 % due to flow maldistribution and end plate effects altogether.

These considerations are however dependent on the boundary conditions used in the study. Among these, the different superheat and the number of channels could largely affect the outcome of the analysis. The larger number of channels employed for both the mixtures reduced the effect of end plates from -5.2 % for Butane down to less than -1 % for both the mixtures. Moreover, a larger imposed superheat is likely to increase the vapor phase pressure drop, thereby leading to a further reduction of the mass flow in the channels reaching a higher degree of superheat. In order to compare performance under same boundary conditions for the pure and mixed refrigerants, a comparison was carried out between Butane and Propylene/Butane (0.5/0.5) for the same number of channels, e.g. 23, and the same controlled value for superheat e.g. 5 K. The plate geometry was kept constant as presented in Table 2.

Figure 5 (a) shows the obtained refrigerant mass flow distribution of Propylene/Butane (0.5/0.5). Compared to the results of Butane (Figure 2 (a)), the same trend was obtained. As expected, the larger superheat implied a reduction of the refrigerant mass flow rate for the channels with higher inlet vapor quality, reaching the superheated region earlier. It is however shown that the magnitude of this effect is much lower in the case of the mixture compared to the pure fluid, with maximum percentage deviations of the mass flow rate of – 5.8 % from the average, in the case of $\Delta x = 0.25$, against the +46.7 % of Butane, as reported in the first two columns of Table 5.

The mass distribution effect was translated into heat transfer performance degradation, as shown in Figure 5 (b) for the case of Propylene/Butane (0.5/0.5). The trend is similar to the one of Butane (shown in Figure 4 (a)), with a first decrease in the total heat flow rate due to the effect of end plates, and a further decrease in performance when a larger non-uniform vapor quality distribution was imposed at the inlet. The percentage deviations are reported in the last four columns of Table 5 using the 1D-model results as reference case. Propylene/Butane (0.5/0.5) experienced a degradation of heat transfer due to end plates equal to around 1/3 of the same effect for the pure fluid. The degradation due to non-uniform quality distribution was smaller, causing an additional -0.4% loss in total heat flow rate. Butane, on the other hand was largely influenced by both end plates and the maldistribution, leading to an equal degradation of heat transfer, around -6 % for each.
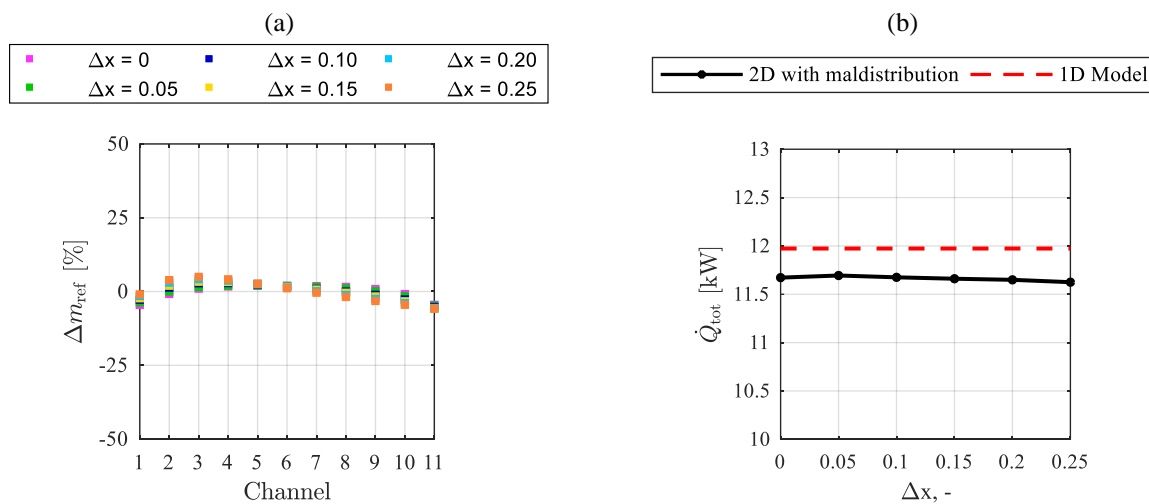
Figure 5: (a) Deviation from average refrigerant mass flow rate in each channel and (b) total heat flow rate as function of the maldistribution rate for Propylene/Butane (0.5/0.5) with 23 total channels and 5 K superheat

Table 5: Mass flow maximum deviations and maximum estimated degradation of total heat flow rate due to end plates and to liquid/vapor maldistributions for Butane and Propylene/Butane (0.5/0.5)

Working fluid	$\dot{m}_{ref_{tot}}$, ($\Delta x = 0.25$), kg/s	max($\Delta\dot{m}_{ch}$) ($\Delta x = 0.25$), %	$\dot{Q}_{tot}$ (1D – ref.), kW	$\dot{Q}_{tot}$ ($\Delta x = 0$), kW	$\Delta\dot{Q}_{tot}$, %	$\dot{Q}_{tot}$ ($\Delta x = 0.25$), kW	$\Delta\dot{Q}_{tot}$, %
Butane	0.0334	+ 46.7	11.8	11.2	- 6.3	10.4	- 11.2
Propylene/Butane (0.5/0.5)	0.0349	- 5.8	12.0	11.7	- 2.5	11.6	- 2.9

5.2 Limitations and future work

The flow distribution was solved by imposing equal pressure drops of both fluids across the channels, thereby entailing a strong dependence of the results on the chosen empirical correlation for the frictional contribution to pressure drop. The study was however carried out by applying the same model to pure fluid and mixtures, and hence led to a reasonable comparison between the fluids, regardless of the uncertainties in the calculation. Investigating the effect of using alternative correlations would be a further step to validate the present results. Moreover, the study was carried out for a specific application of a booster heat pump for a DH network, thus further validation would be obtained by evaluating additional refrigerants and different operating conditions for various applications. Last, the economic benefit of PHE performance entailed by mixture utilization, avoiding a likely degradation of the heat pump COP, could be compared with the increasing investment due to larger required heat transfer area.

5. CONCLUSIONS

The impact of uneven liquid/vapor distribution at the inlet of a PHE evaporator was evaluated for the case study of a booster heat pump for a DH network. Three different refrigerants were compared, namely Butane, Propylene/Butane (0.5/0.5) and R1234yf/R1233zdE (0.5/0.5). The degradation of PHE performance was evaluated for different cases of maldistribution, imposed by assuming a linear variation of the inlet vapor quality across the PHE channels. Butane was the most affected by maldistribution, with a consistent reduction of the mass flow rates in the channels with higher inlet quality, reaching the superheated region earlier. A degradation of the heat flow rate equal to - 6.3 % was estimated as the sole effect of end plates, while an overall reduction of - 11.2% was estimated in case of severe maldistribution. Both zeotropic mixtures were only slightly affected by end plates, with heat transfer rate decrease of - 0.9% and - 0.8 %, while the uneven vapor/quality distribution resulted in a negligible effect on the total heat flow rate.

NOMENCLATURE

COP	coefficient of performance	(-)	$\dot{Q}$	heat flow rate	(kW)
L	plate length	(m)	T	temperature	(K or °C)
$\dot{m}$	mass flow rate	(kg/s)	$\dot{V}$	volume flow rate	(m^3/hr)
N_{ch}	number of channels	(-)	W	plate width	(m)
p	pressure	(bar)	x	vapor quality	(-)

Greek letters

Δ	difference	(-)	ρ	density	(kg/m^3)

Subscripts

ch	channel		out	outlet
eva	evaporator		ref	refrigerant
hs	heat source		sh	superheating
in	inlet		tot	total

REFERENCES

Amalfi, R., Vakili-Farahani, F., Thome, J., 2016. Flow boiling and frictional pressure gradients in plate heat exchangers part 2 Comparison of literature methods to database and new prediction methods. Int. J. Refrig. 61, 185–203.

Bassiouny, M.K., Martin, H., 1984a. Flow distribution and pressure drop in plate heat exchangers—I U-type arrangement. Chem. Eng. Sci. 39, 693–700. https://doi.org/10.1016/0009-2509(84)80176-1

Bassiouny, M.K., Martin, H., 1984b. Flow distribution and pressure drop in plate heat exchangers—II Z-type arrangement. Chem. Eng. Sci. 39, 701–704.

Bell, I.H., Wronski, J., Quoilin, S., Lemort, V., 2014. Pure and pseudo-pure fluid thermophysical property evaluation and the open-source thermophysical property library coolprop. Ind. Eng. Chem. Res. 53, 2498–2508.

Bell, K., Ghaly, M., 1973. An approximate generalized design method for multicomponent/partial condenser. AIChE Symp. Ser. 69, 72–79.

Bobbili, P.R., Sunden, B., Das, S.K., 2006. An experimental investigation of the port flow maldistribution in small and large plate package heat exchangers. Appl. Therm. Eng. 26, 1919–1926.

Collier, J.G., Thome, J.R., 1994. Convective boiling and condensation, (3rd Ed.), Oxford University Press.

Cooper, M.G., 1984. Heat flow rates in saturated nucleate pool boiling - a wide ranging examination using reduced properties. Adv. Heat Transf. 16, 59–156.

Jensen, J.K., Kaern, M.R., Ommen, T.S., Brix, W., Reinholdt, L., Elmeegard, B., 2015. Effect of liquid/vapour maldistribution on the performance of plate heat exchanger evaporators, in: Proceedings of the 24th IIR International Congress of Refrigeration.

Jin, S., Hrnjak, P., 2017a. Effect of end plates on heat transfer of plate heat exchanger. Int. J. Heat Mass Transf. 108, 740–748. https://doi.org/10.1016/j.ijheatmasstransfer.2016.11.106

Jin, S., Hrnjak, P., 2017b. A new method to simultaneously measure local heat transfer and visualize flow boiling in plate heat exchanger. Int. J. Heat Mass Transf. 113, 635–646.

Lemmon, E.W., Huber, M.L., McLinden, M.O., 2013. NIST Standard Reference Database 23. Ref. Fluid Thermodyn. Transp. Prop. (REFPROP), Version 9.1.

Li, W., Hrnjak, P., 2016. Single Phase Pressure Drop and Flow Distribution in Brazed Plate Heat Exchangers, in: International Refrigeration and Air Conditioning Conference. Purdue university, p. Paper 1812.

Lockhart, R.W., Martinelli, R.C., 1949. Proposed correlation of data for isothermal two-phase, two-component flow in pipes. Chem. Eng. Prog. 45, 39–48.

Martin, H., 1996. A theoretical approach to predict the performance of chevron-type plate heat exchangers. Chem. Eng. Process. Process Intensif. 35, 301–310. https://doi.org/10.1016/0255-2701(95)04129-X

Mathworks, 2017. fsolve, Matlab 2017b URL https://www.mathworks.com (accessed 3.5.18).

Mueller, A.C., Chiou, J.P., 1988. Review of various Types of Flow Maldistribution in Heat Exchangers. Heat Transf. Eng. 9, 36–50. https://doi.org/10.1080/01457638808939664

Palm, B., Claesson, J., 2006. Plate Heat Exchangers: Calculation Methods for Single and Two-Phase Flow. Heat Transf. Eng. 27, 88–98. https://doi.org/10.1080/01457630500523949

Radermacher, R., Hwang, Y., 2005. Heat Transfer of Refrigerant Mixturers, in: Vapor Compression Heat Pumps with Refrigerant Mixtures. CRC Press 2005, pp. 237–278. https://doi.org/doi:10.1201/9781420037579.ch8

Rao, B.P., Das, S.K., 2004. An Experimental Study on the Influence of Flow Maldistribution on the Pressure Drop Across a Plate Heat Exchanger. J. Fluids Eng. - Trans. ASME 126, 680–691. https://doi.org/10.1115/1.1779664

Rao, B.P., Sunden, B., Das, S.K., 2005. An Experimental and Theoretical Investigation of the Effect of Flow Maldistribution on the Thermal Performance of Plate Heat Exchangers. J. Heat Transf. Asme 127.

Shah, R.K., Sekulic, D.P., 2002. Fundamentals of Heat Exchanger Design, … to Thermo-Fluids Systems Design.

Silver, L., 1947. Gas cooling with aqueous condensation. Ind. Chem. Chem. Manuf. 23, 380–386.

Smith, S.L., 1969. Void fractions in two-phase flow: a correlation based upon an equal velocity head model. Proc. Inst. Mech. Eng. 184, 647–664. https://doi.org/10.1243/PIME_PROC_1969_184_051_02

SWEP International AB, 2015. SWEP Products URL https://www.swep.net/products/ (accessed 2.23.18).

Tereda, F.A., Srihari, N., Sunden, B., Das, S.K., 2007. Experimental investigation on port-to-channel flow maldistribution in plate heat exchangers. Heat Transf. Eng. 28, 435–443.

Thome, J.R., Shakir, S., 1987. A new correlation for nucleate pool boiling of aqueous mixtures. AIChE Symp. Ser. 83, 46–51.

Vist, S., Pettersen, J., 2004. Two-phase flow distribution in compact heat exchanger manifolds. Exp. Therm. Fluid Sci. 28, 209–215. https://doi.org/10.1016/S0894-1777(03)00041-4

Zhang, J., Desideri, A., Kærn, M.R., Ommen, T.S., Wronski, J., Haglind, F., 2017. Flow boiling heat transfer and pressure drop characteristics of R134a, R1234yf and R1234ze in a plate heat exchanger for organic Rankine cycle units. Int. J. Heat Mass Transf. 108, 1787–1801. https://doi.org/10.1016/j.ijheatmasstransfer.2017.01.026

Zühlsdorf, B., Meesenburg, W., Ommen, T., Kjaer Jensen, J., Brix Markussen, W., Elmegaard, B., 2018. Improving the performance of booster heat pumps using zeotropic mixtures. Energy.

ACKNOWLEDGEMENT